Supporting Information

McPherson et al. 10.1073/pnas.0905524107

SI Materials and Methods

Animal Feed, Housing, and Hormone Analysis. TNFαKO and Balb-c/Nude mice were fed regular feed (10% soy meal), ArKO mice fed soy-free feed (Glen Forrest Stockfeeders) and NOD/SCID mice were fed Picodiet 5053 (PMI Nutrition International), with ad libitum access to water. All animals were housed in specific pathogen-free conditions according to National Health and Medical Research Council, Australia and National Institutes of Health guidelines. Studies were approved by Animal Ethics Committees at Monash University or BC Cancer Research Centre. Serum testosterone levels were measured by ANZAC Research Institute (Sydney, Australia) as previously described (1).

Enriching for CD133$^+$ Stem/Progenitor Cells. Cell lines were fractionated using previously published protocols (2, 3). The CD133$^+$ fraction was shown to be 99% pure by immunohistochemistry. Cell treatments were as described in *Materials and Methods.*

Knockdown of ERβ and TNFα by Specific siRNA. Reverse transfection of DU145 cells was performed with siRNA oligonucleotides; cells were plated in multichambered slides or six-well plates for cleaved caspase-3 immunohistochemistry or RNA extraction, respectively. The cells were transfected while still in suspension (i.e., after trypsinization and before plating) with 50 nM siRNA from the siGENOME SMARTpool (Dharmacon) using Lipofectamine 2000 (Invitrogen), according to the manufacturer's instructions. Cells were also transfected with nontarget siRNA to ensure the specificity of siRNA. Twenty-four hours posttransfection, medium was replaced with fresh culture medium. Seventy-two hours posttransfection, cells were incubated with 6 μM ERβ agonist or vehicle control for another 12 h, and subsequently analyzed for cleaved caspase 3 using unbiased stereological methods.

RT-PCR Analysis of ERβ and TNFα Transcript Levels. Seventy-two hours posttransfection, total RNA was extracted using RNeasy Mini Kit (Qiagen) according to the manufacturer's instructions. RT was performed as previously described (4). Absolute quantitative real-time analysis was used to assess the levels of mRNA expression in transfected cells. The analysis was performed on Applied Biosystems 7900HT Fast Real-time PCR system (Applied Biosystems) using Power SYBR Green PCR Master Mix (Applied Biosystems) according to the manufacturer's instructions. The quantity of mRNA was determined using a standard curve, and all values were normalized using the house keeping gene, ribosomal L32 gene. Primer sequences were as follows: ERβ Forward-TGTCTGCAGCGATTACGCA, Reverse-GCGCCGGTTTTT-ATCGATT, TNFα Forward- TCAATCGGCCCGACTATCTC, Reverse-CAGGGCAATGATCCCAAAGT and L32 Forward-CAGGGTTCGTAGAAGATTCAAGGG, Reverse-CTTGAG-GAAACATTG TGAGCGATC.

Prostate Tissues and Xenografting. Specimens were obtained from four men with BPH and three men with PCa undergoing transurethral resections or radical prostatectomy at Vancouver General Hospital, as approved by the University of British Columbia Clinical Research Ethics Board. BPH specimens were evaluated by a pathologist to confirm the presence of benign and the absence of malignant prostate tissue. Cancer specimens, identified on gross morphological assessment of tumor margins by the surgeon, were confirmed by urologic pathology as Gleason Score 7 and shown by us to express ERβ immunoreactivity (Fig. S8). For xenografting, each independent patient specimen was divided into smaller pieces, each of which was grafted into a minimum of two host male NOD-SCID mice/treatment (i.e., a minimum of six mice per patient, with two to four grafts per mouse). After 4 weeks of xenograft establishment, host mice were randomly sorted into three treatment groups (Control, Castrate, and ERβ agonist) and treated for 3 days, after which tissues were harvested.

Treatment of Grafted PC3 Tumors in Vivo. DsRed tagged fluroscent PC3 cells (gifted by Elizabeth D. Williams, Monash Institute of Medical Research) were s.c. injected (2.5×10^5 cells) in BALB/c nude mice. Two weeks after cell inoculation, animals were imaged using in vivo fluorescent imaging and were subsequently imaged twice a week. Tumor progression was determined by measuring fluorescence intensity using Fujifilm Multi Gauge software (Fujifilm Life Science Systems). The animals were then randomly sorted into ERβ agonist treatment ($n = 7$) and vehicle treatment groups ($n = 6$). The ERβ agonist treatment group received 300 μg/kg/day ERβ agonist, whereas the vehicle treatment group received equivalent 100% ethanol in carrier for 5 weeks. After this, mice were euthanized. Tumors were then harvested, weighed, measured with calipers, and fixed for IHC for detection of apoptosis and proliferation.

ApopTag and Dual Immunofluorescence Staining of Paraffin Sections. Slides were prepared as for immunohistochemistry. Sections were then incubated with CKH (DAKO) or cleaved Caspase 3 (Cell Signaling) and ERβ (Novocastra) for 1 h. Following washes, sections were stained with anti-mouse IgG1-Alexa555, anti-rabbit IgG-Alexa488, or anti-mouse IgG1-Alexa633, respectively (1:500 dilution; Invitrogen). Sections were washed and then stained for apoptosis using the fluorescent ApopTag kit (Chemicon) as per the manufacturer's instructions, or stained for CD133 (Abcam; secondary antibody was anti-rabbit IgG-Alexa555) and mounted with Vectashield-DAPI (Vector Laboratories). All sections were examined using a Nikon A1 Rsi confocal microscope (Nikon, Japan) with lasers exciting at 402, 488, and 638 (emission detection at 425–475, 570–620, and 662–737). Multicolor images were collected sequentially in three channels and captured using the Nikon NIS Elements imaging software.

Quantification of Immunostaining. Using a systematic uniform random sampling scheme, at least six to 12 tissue sections/prostate were selected for IHC staining (see above). Once stained, quantification of tissue immunoreactivity was performed using a Bioprecision2 Microscope Stage (LUDL), 99A400 Focus drive (LUDL), MAC5000 Controller (LUDL) and ND-281 Encoder (Heidenhain) coupled to an Olympus BX-51 microscope (Olympus). The images were captured using a PixeLink PL-623C digital camera (PixeLink) coupled to a computer. The newCAST component (version 2.14; Visiopharm) of the Visiopharm Integrator System (version 2.16.1.0; Visiopharm) was used to generate a set of counting frames and a point grid (grid properties were assessed individually for each marker).

Uniform systematic random sampling was then used to quantitate the number of positive and negative cells, as previously described (1, 5, 6). In brief, sections were examined at ×10 magnification, mapped to define tissue boundaries, and sampled at predetermined intervals along the *x* and *y* axes using a single-point grid-counting frame to allow sampling of 5% of the selected tissue sections. Using brightfield imaging, under ×40 magnification, positive cells were scored and totaled for each respective tissue, with the results expressed as a percentage of total cells counted.

For separation of epithelium into basal and luminal cells, identification was based on morphological criteria, basal cell morphology ranging from small flattened cells with condensed chromatin and scant cytoplasm to more cuboidal cells with increased amounts of cytoplasm adjacent to the basement membrane; luminal cells were identified by their columnar appearance with apical aspect projecting into the prostatic lumen. Identification of apoptotic basal cells was confirmed by dual fluorescent labeling of Apoptag and CKH in selected serial sections. A similar stereological methodology was repeated for in vitro studies on prostate cell lines. Borders of wells were mapped, and 25% of each well was sampled to allow assessment of a minimum of 1,000 cells/well per treatment, with numbers of immuno-positive and -negative cells counted and expressed as a percentage of total cells counted.

Quantification of Cystic Atrophy. Atrophic regions were identified using morphologic criteria, including loss of epithelial cells, loss of epithelial cell height/reduction in epithelial cytoplasm, and expansion of luminal space because of increased secretory fluid. The percent area of atrophy after recovery from treatment was determined using >10 uniformly randomly selected sections. Subsequent mapping and analysis of normal and atrophic regions in VIS allowed the area of atrophic regions to be defined and compared with areas of normal morphology within each prostate tissue to provide a percentage value of the extent of atrophy within a tissue.

Oligo Gene Expression Array. Analysis of GEArray DNA microarray (OMM-012; SuperArray Bioscience Corp.) was conducted on a minimum of four samples per group in duplicate and at two different time points, i.e., 12 h or 3 days of treatment. Data analysis was conducted using GEArray Expression Analysis Suite (SuperArray Bioscience), with expression normalized to a specific set of housekeeping genes [ribosomal protein L32 (*Rpl32*), lactate dehydrogenase A (*Ldha*), glyceraldehyde 3-phosphate dehydrogenase (*Gadph*), peptidylprolyl isomerase A (*Ppia*)].

1. McPherson SJ, et al. (2007) Essential role for estrogen receptor beta in stromal-epithelial regulation of prostatic hyperplasia. *Endocrinology* 148:566–574.
2. Richardson GD, et al. (2004) CD133, a novel marker for human prostatic epithelial stem cells. *J Cell Sci* 117:3539–3545.
3. Collins AT, Habib FK, Maitland NJ, Neal DE (2001) Identification and isolation of human prostate epithelial stem cells based on alpha(2)beta(1)-integrin expression. *J Cell Sci* 114:3865–3872.
4. Balanathan P, et al. (2004) Epigenetic regulation of inhibin alpha-subunit gene in prostate cancer cell lines. *J Mol Endocrinol* 32:55–67.
5. Bianco JJ, McPherson SJ, Wang H, Prins GS, Risbridger GP (2006) Transient neonatal estrogen exposure to estrogen-deficient mice (aromatase knockout) reduces prostate weight and induces inflammation in late life. *Am J Pathol* 168:1869–1878.
6. Bianco JJ, Handelsman DJ, Pedersen JS, Risbridger GP (2002) Direct response of the murine prostate gland and seminal vesicles to estradiol. *Endocrinology* 143:4922–4933.

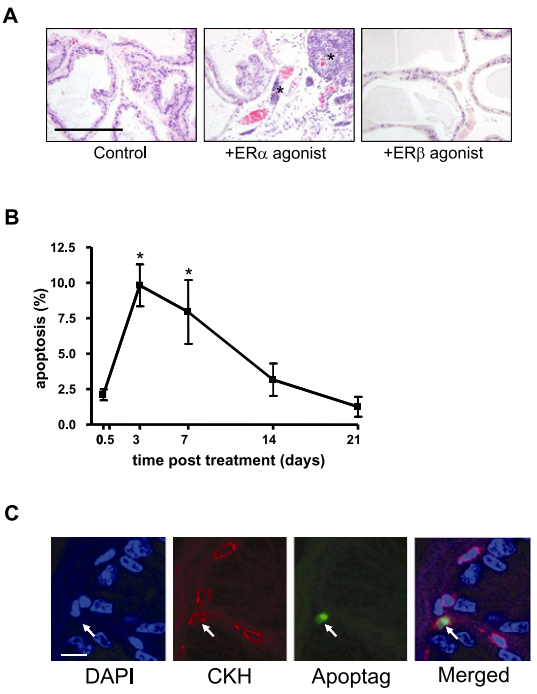

Fig. S1. (*A*) ERα agonist–induced inflammation in ArKO mouse prostate. After 6 weeks' treatment with vehicle or ERα agonist, there was accumulation and infiltration of inflammatory cells in ventral prostate tissue that was not observed in vehicle- or ERβ-agonist–treated mice. *Areas of inflammation. (Scale bar, 200 μm.) (*B*) Time course showing percent apoptosis in ArKO mice treated with ERβ agonist. *$P < 0.05$, $n > 3$ per group. (*C*) Representative tissue section showing apoptosis in basal cells. Immunofluorescent colocalization of the basal cell marker CKH with ApopTag staining after ERβ treatment. Arrow shows dual labeled basal cell undergoing apoptosis. (Scale bar, 10 μm).

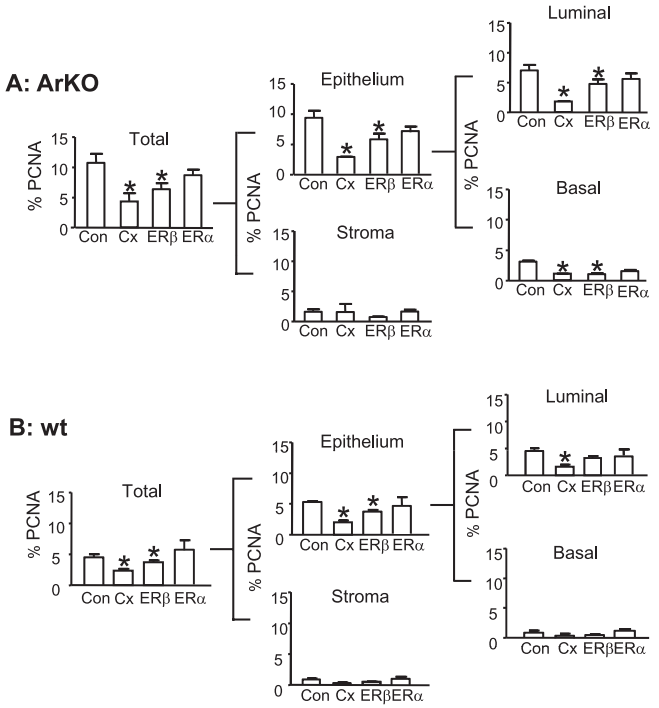

Fig. S2. Effect of selective ERβ agonist on prostatic proliferation in ArKO and wt mice. ERβ agonist-induced anti-proliferative effects in (*A*) ArKO or (*B*) wt prostate tissues (determined by PCNA immunolocalization) in total tissue, subdivided into epithelial (luminal or basal) and stromal components at 3 days from control (Con), castration (Cx), ERβ agonist (ERβ), or ERα agonist (ERα). Values are mean ± SEM; $n = 5$ animals per group. nd, not detectable.*$P < 0.05$ vs. control.

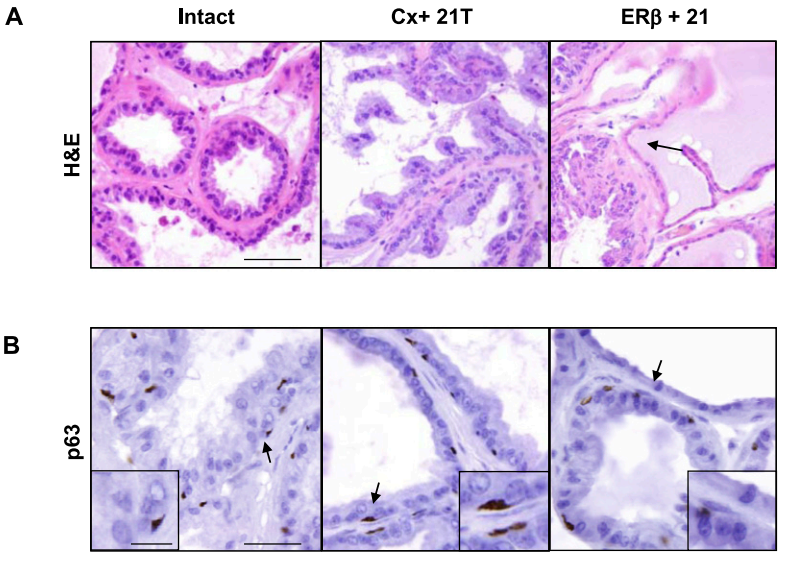

C

	Control	Cx	Cx+21T	ERβ	ERβ+21	
					Non-atrophic	atrophic
p63+ frequency (%)	11.6 ± 1.9	10.2 ± 0.9	10.2 ± 1.2	9.2 ± 0.6	9.8 ± 1.2	4.9 ± 1.4*

Fig. S3. Recovery of prostatic structure and function after ERβ agonist treatment was different from castration recovery. (*A*) H&E-stained sections showing similar appearance of control and castrate tissue after 21 days T replacement (Cx+21T) compared with cystic atrophy (arrow) in ERβ-treated tissues 21 days posttreatment (ERβ+21). (*B*) Immunolocalization of basal cell marker p63 identifies basal cells in intact, Cx+21T, and ERβ+21 tissues and indicates a reduced frequency of p63-stained cells in regions of cystic atrophy in ERβ+21 prostate tissues. (*C*) Frequency of p63+ basal cells/100 epithelial cells in normal and/or regions of cystic atrophy after 3 day treatment with or without 21-day recovery. Values represent mean ± SEM; $n = 3$–5 per group. *$P < 0.05$ vs. control. (Scale bar, *A,* 50 μm; *B* and *Inset,* 20 μm.)

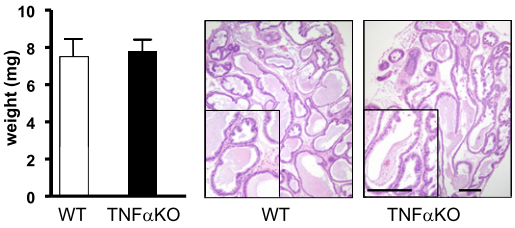

Fig. S4. Characterization of TNFαKO mouse prostate. Weights of ventral prostates from untreated TNFαKO mice were not significantly different from those of age-matched wt mice. No overt evidence of altered morphology could be observed in TNFαKO prostates, which were comparable to wt tissues. (Scale bar, 200 μm.)

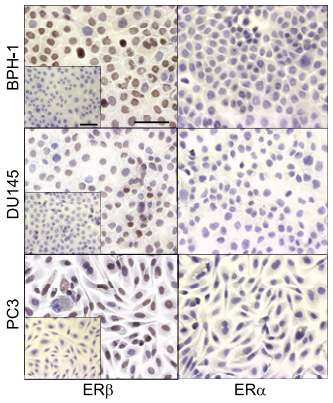

Fig. S5. Immunolocalization of estrogen receptors, ERβ and ERα, in human prostate cell lines. Immunoreactivity for ERβ was detected in benign (BPH-1) and malignant (DU145 and PC3) cell lines, whereas ERα was undetectable in all cell lines. (*Inset*) Negative control. (Scale bar, 200 μm).

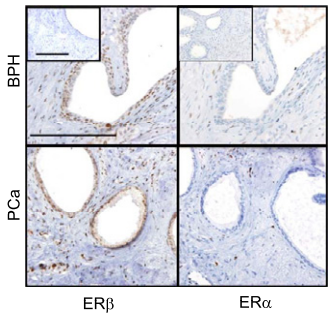

Fig. S6. Immunolocalization of estrogen receptors, ERβ and ERα, in vehicle-treated human BPH and PCa tissue xenografts. Immunoreactivity for ERβ was detectable in epithelium and stroma of BPH and PCa specimens, whereas ERα immunoreactivity was limited to a small number of cells, primarily in the stroma. (*Inset*) Negative control. (Scale bar, 200 μm).

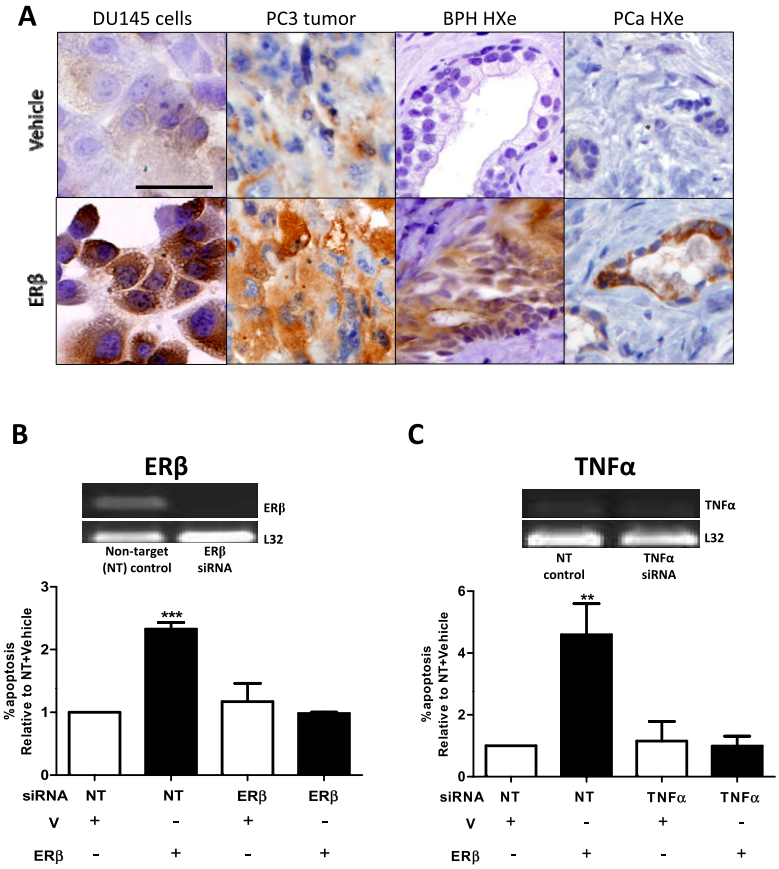

Fig. S7. TNFα expression in human tissues and siRNA knockdown studies in DU145 cells. (*A*) Immunoreactivity for TNFα was detectable in all ERβ-agonist–treated tissues (including DU145 cells treated in vitro for 12 h, s.c. xenografts of PC3 cells, or subrenal xenografts of human BPH or PCa specimens), and was undetectable or limited in vehicle-treated tissues. Cells were transfected with 50 nM siRNA against ERβ (*B*), TNFα (*C*), or nontarget control (*B* and *C*). After 72 h of incubation, total RNA was extracted and RT-PCR was performed to show knockdown of ERβ (*B*) and TNFα (*C*). Proapoptotic effects of vehicle (open bars) and ERβ agonist (closed bars) on siRNA knockdown DU145 cells was analyzed using expression of cleaved caspase-3. (Scale bar, 200 μm.) Values are mean ± SEM, n = 4 wells/treatment for *B*. $^{**}P < 0.005$ vs. vehicle control. $^{***}P < 0.0005$ vs. vehicle control.

Table S1. Serum testosterone levels (nM) of ArKO mice

	Control	Cx	ERβ	ERα
3 days	13.84 ± 2.89	0.14 ± 4.29*	18.72 ± 3.47	15.89 ± 4.41
3 + 21 days	16.48 + 3.33	9.10 ± 5.83†	12.46 ± 2.82	11.72 ± 3.87

Serum testosterone levels (nM) of ArKO mice after 3-day treatment or 3-day treatment plus 21-day recovery: Control (vehicle treated), Castration (CX), ERβ agonist (βSERM), or ERα agonist (ERα). Values represent mean ± SEM; n = 5–12 per group.
*$P < 0.05$ vs. control.
†Testosterone replacement.

Table S2. Gene expression during ERβ agonist or castration induced apoptosis in ArKO mice

			12-h treatment		3-day treatment	
RefSeq number	Symbol	Description	Cx/intact	ERβ/intact	Cx/intact	ERβ/intact
NM_013693	Tnf	Tumor necrosis factor	1.22	1.84	1.64	6.42
NM_020275	Tnfrsf10b	Tumor necrosis factor receptor superfamily, member 10b	1.09	2.20	1.44	3.31
NM_008764	Tnfrsf11b	Tumor necrosis factor receptor superfamily, member 11b	1.03	2.09	1.33	2.99
NM_013749	Tnfrsf12a	Tumor necrosis factor receptor superfamily, member 12a	0.92	1.89	2.27	4.43
NM_178931	Tnfrsf14	Tumor necrosis factor receptor superfamily, member 14	1.24	2.09	2.29	5.36
NM_011609	Tnfrsf1a	Tumor necrosis factor receptor superfamily, member 1a	1.44	2.06	1.18	3.55
NM_178589	Tnfrsf21	Tumor necrosis factor receptor superfamily, member 21	1.38	1.76	0.99	2.56
NM_023680	Tnfrsf22	Tumor necrosis factor receptor superfamily, member 22	1.19	1.78	0.81	2.62
NM_011611	Cd40	CD40 antigen	0.87	1.94	1.34	3.77
NM_007987	Fas	Fas (TNF receptor superfamily member)	0.97	2.17	1.23	2.86
NM_009425	Tnfsf10	Tumor necrosis factor (ligand) superfamily, member 10	1.15	2.51	1.35	2.70
NM_011614	Tnfsf12	Tumor necrosis factor (ligand) superfamily, member 12	1.44	2.84	1.82	3.01
NM_019418	Tnfsf14	Tumor necrosis factor (ligand) superfamily, member 14	1.27	2.11	2.14	4.40
NM_01161.6	Cd40lg	CD40 ligand	1.26	1.91	1.13	3.45
NM_010177	Fasl	Fas ligand (TNF superfamily, member 6)	1.44	1.78	1.07	2.63
NM_009421	Traf1	Tnf receptor-associated factor 1	1.31	1.78	0.75	2.05
NM_009422	Traf2	Tnf receptor-associated factor 2	0.91	1.83	1.51	3.61
NM_011632	Traf3	Tnf receptor-associated factor 3	0.85	1.84	1.18	2.70
NM_009423	Traf4	Tnf receptor associated factor 4	1.12	2.42	1.39	2.64
NM_011633	Traf5	Tnf receptor-associated factor 5	1.13	2.92	1.67	2.64
NM_011640	Trp53	Transformation related protein 53	2.05	2.29	1.48	2.95
NM_173378	Trp53bp2	Trp53 binding protein 2	1.02	1.34	1.02	3.02
NM_021897	Trp53inp1	Trp53 inducible nuclear protein 1	1.08	1.14	0.80	2.51
NM_011642	Trp73	Transformation related protein 73	1.08	1.86	1.07	2.44

Gene expression during ERβ agonist- or castration-induced apoptosis in ArKO mice. Comparison of the ratio of fold changes of key apoptotic proteins in castrate:intact compared with ERβ agonist:intact following 12-h or 3-day treatment.

Table S3. Characterization of in vivo PC3 tumor response to ERβ agonist treatment and change in doubling time

	Δt (fold change)	Percent apoptosis	Percent proliferation
+ Vehicle	1.78 ± 0.35	0.48 ± 0.11	12.9 ± 1.3
+ ERβ agonist	3.38 ± 0.61	0.79 ± 0.06*	8.0 ± 1.4*

Characterization of in vivo PC3 xenograft tumor response to ERβ agonist treatment including fold increase of doubling time, apoptosis, and proliferation.
*$P < 0.05$ vs. vehicle, n = 4–8.